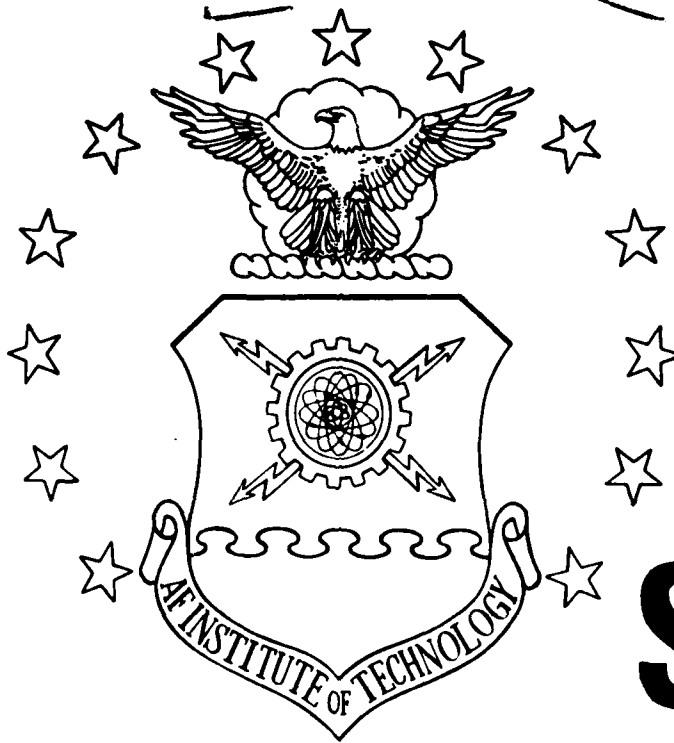


MICROCOPY RESOLUTION TEST CHART
NATIONAL BUREAU OF STANDARDS 1963 A

AD-A163 838



DTIC
ELECTE
FEB 11 1986
S D

QUANTUM THEORY OF ION MOTION AND LASER CO
IN A RADIO FREQUENCY QUADRUPOLE TRAP

THESIS

Ann Laurie Wells
Captain, USAF

AFIT/GEP/PH/84D-12

DISTRIBUTION STATEMENT A

Approved for public release;
Distribution Unlimited

DTIC FILE COPY

DEPARTMENT OF THE AIR FORCE
AIR UNIVERSITY
AIR FORCE INSTITUTE OF TECHNOLOGY

Wright-Patterson Air Force Base, Ohio

AFIT/GEP/PH/84D-12

①

DTIC
ELECTE
S FEB 1 1 1986 **D**
D

QUANTUM THEORY OF ION MOTION AND LASER COOLING
IN A RADIO FREQUENCY QUADRUPOLE TRAP

THESIS

Ann Laurie Wells
Captain, USAF

AFIT/GEP/PH/84D-12

Approved for public release; distribution unlimited.

AFIT/GEP/PH/84D-12

QUANTUM THEORY OF ION MOTION AND LASER COOLING
IN A RADIO FREQUENCY QUADRUPOLE TRAP

THESIS

Presented to the Faculty of the School of Engineering
of the Air Force Institute of Technology
Air University
in Partial Fulfillment of the
Requirements for the Degree of
Master of Science

Ann Laurie Wells, B.S.
Captain, USAF

December 1984

Accession For	
NTIS CRA&I	<input checked="" type="checkbox"/>
DTIC TAB	<input type="checkbox"/>
Unannounced	<input type="checkbox"/>
Justification	
By	
Distribution/	
Availability Codes	
Dist	Avail and/or Special
A-1	

Approved for public release; distribution unlimited.



Acknowledgements

The author wishes to thank the members of the faculty at AFIT who particularly helped with this work: Maj. Cook of the Physics Department for many enlightening conversations and constant encouragement and Dr. Lee of the Mathematics Department for his helpful discussions on Mathieu functions. I also wish to thank Jay T. Wells for more assistance than it is possible to describe.

ANN LAURIE WELLS

Table of Contents

Acknowledgements ii

List of Figures iv

Abstract v

I. Introduction 1

 Purpose and Scope 1

 Background 2

II. Ion Motion in the Absence of Laser Cooling 8

 Effective Potential Solution 8

 Wave Packet Solution 12

III. The Laser Cooling Process 20

 Hamiltonian Matrix Elements 20

 Development of Density Matrix Equations 29

IV. Conclusion 37

Bibliography 39

Appendix 41

Vita 42

List of Figures

<u>Figure</u>		<u>Page</u>
1	Radio Frequency Quadrupole Trap With Laser Cooling Arrangements	3
2	Energy Level Diagram for Laser Cooling Arrangements	6
3	Graph of Width Versus Time for Experimental Parameters	16
4	Graph of Width Versus Time for $\Omega = 10\Omega_0$	17
5	Graph of Width Versus Time for $\Omega = \Omega_0$	18
6	Energy Levels and Transitions of the Ionic System in the Quadrupole Trap	21

$\psi = (1 - \epsilon) \cos(\Omega \text{e} V_0 \times t)$

Abstract

The problem of ion motion and laser cooling in a radio frequency quadrupole trap is considered. It is shown by a simple numerical calculation that for ion motion in the absence of laser cooling the effect of the time varying potential $\psi(\vec{R}) \cos \Omega t$ can be approximated by a time independent effective potential whenever the frequency of oscillation of the electric field, Ω is sufficiently greater than a resonant frequency, $\Omega_0 = \sqrt{2} e V_0 / M$, where e is the electronic charge, V_0 is the maximum potential applied to the trap electrodes, and M is the mass of the ion.

Equations for the Hamiltonian matrix elements in the presence of laser cooling, in the Lambe-Dicke limit are derived and studied to determine the cooling transitions. The equations of motion for the density matrix in the Lambe-Dicke limit are derived using a simple representation of spontaneous emission.

$\Omega_0 = \sqrt{2} e V_0 / M$

QUANTUM THEORY OF ION MOTION AND LASER COOLING
IN A RADIO FREQUENCY QUADRUPOLE TRAP

I. Introduction

Purpose and Scope

A radio frequency quadrupole trap coupled with laser cooling has been used to trap a single ion and hold it in a volume with dimensions of $2\mu\text{m}$ indefinitely (16). The purpose of this thesis is to develop the theory of particle motion in the trap and to determine the mechanisms of the laser cooling process.

Section II of the thesis explores the problem of ion motion in the absence of laser cooling. In particular, conditions for stable trapping are examined. Two approaches to this problem are taken. In the first approach an effective potential is derived. The effective potential solution is derived starting with the actual time varying potential in Schrodinger's equation, instead of starting with the classically derived effective potential as all of the theoretical developments up until now have done (4). The second approach postulates a wave packet solution. An

equation for the width of the packet is derived and explored both analytically and numerically.

Section III of the thesis analyzes the laser cooling process particularly during the final stages when the ion is in the Lamb-Dicke limit, that is, when the width of the ionic wave packet is small compared to the wavelength of the cooling laser. The cooling transitions are determined by evaluating the Hamiltonian matrix elements. The equations of motion for the density matrix elements are derived.

Background

In 1980 Neuhauser, et al. reported trapping a single barium ion in a Paul radio frequency quadrupole trap using laser cooling, and holding it in a volume with dimensions of $2\mu\text{m}$ (16:1137). The trapped, cooled ion can be used for very high resolution spectroscopy. Alone in the trap, its spectral lines will not be broadened by collisions and if it is restricted to a region smaller than $\lambda/4$, the Doppler effect will be suppressed (6:55).

The Paul trap consists of three electrodes: two cap electrodes, shaped like hyperbolas, with a ring electrode between them. An oscillating electric field is applied to the electrodes. The trap is illustrated in Figure 1. The potential created within the trap space is

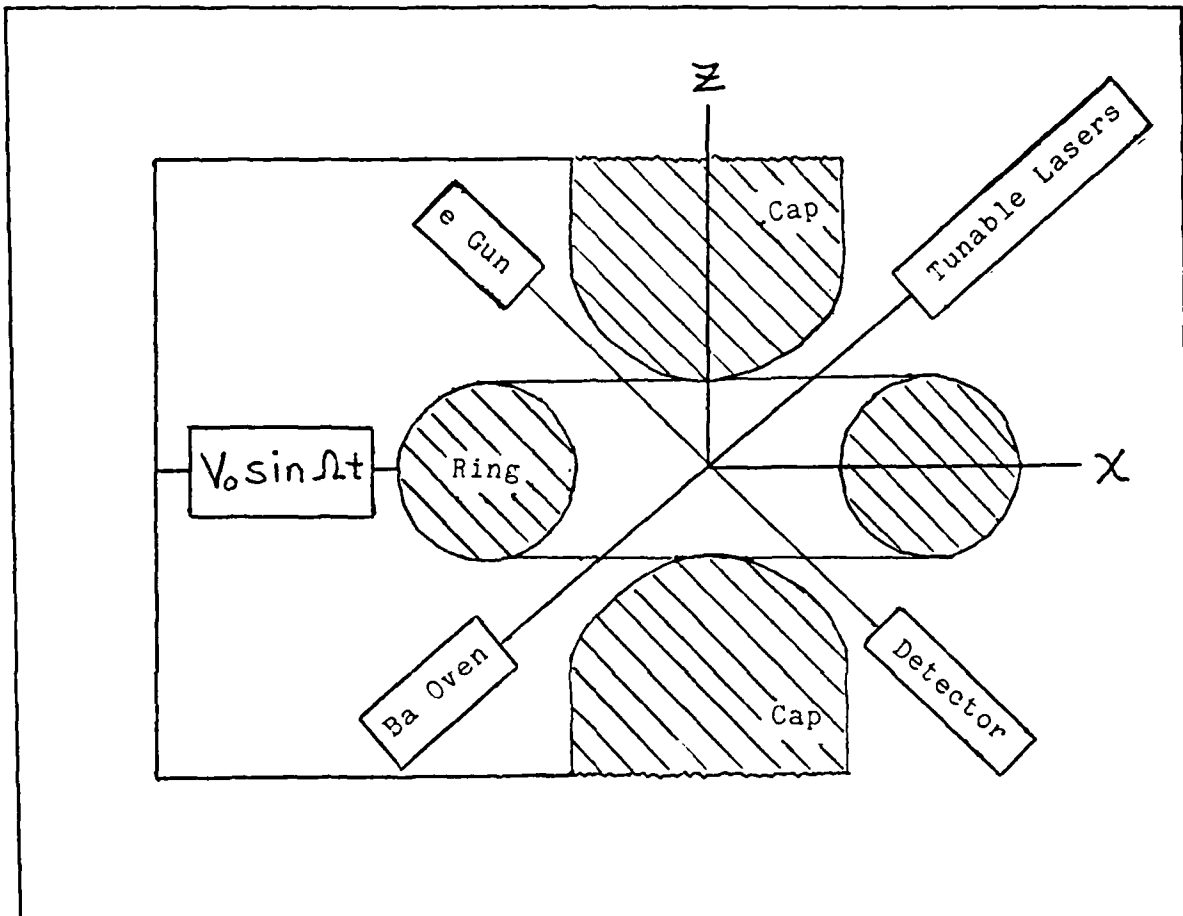


Figure 1. Radio frequency quadrupole trap with laser cooling arrangements.

$$V(\vec{R}, t) = \psi(\vec{R}) \cos \Omega t = V_0 (X^2 + Y^2 - 2Z^2) \cos \Omega t \quad (1)$$

where V is the electric potential, V_0 is a constant, and Ω is the frequency of oscillation of the electric field (6:56-61). The origin of coordinates is at the center of the ring electrode with the Z -axis running between the two cap electrodes, perpendicular to the plane of the ring electrode.

A Paul trap, which has an oscillating electric field, was used instead of a trap with a static electric field, such as a Penning trap, because static traps must use an electric and a magnetic field. The magnetic field causes a Zeeman effect which is undesirable for high resolution spectroscopy (6:55).

In the trap used by Neuhauser, et al., the spacing between the two cap electrodes was 0.5 mm, and the inner diameter of the ring electrode was 0.75 mm. The frequency of oscillation of the electric field, Ω , was $2\pi \times 18$ MHz and the frequency of oscillation of the ion in the well, ν , was $2\pi \times 2.4$ MHz. The barium was injected into the trap from an oven and ionized by an electron beam. The ion was thermalized by allowing helium buffer gas into the trap at a background pressure of $<10^{-4}$ Torr (15:233). A laser tuned to the Ba^+ line at 493.4 nm was shone on the trap, and when a barium ion was present in the trap it could be observed visually by fluorescence (16:1139).

The 493.4 nm line for Ba^+ is a transition between the ground $6^2S_{1/2}$ state and an excited $6^2P_{1/2}$ state. For the purposes of

cooling the ion, the laser was tuned to a frequency below the resonant frequency of the transition by an amount ν . One-third of the time, the ion spontaneously decayed to a $5^2D_{1/2}$ metastable excited state instead of back to the ground state. A second laser, tuned to the $5^2D_{1/2}-6^2P_{1/2}$ transition at 649.9 nm kept the ion from sitting in the metastable state. An energy level diagram is shown in Figure 2. Both laser beams entered the trap between the ring electrode and one of the cap electrodes, at an angle of 45° to the Z -axis.

This experiment generated a flurry of theoretical activity. Several approaches to this problem can be taken: systemising light induced forces (3), (7); investigating the density operator of a particle in a light field (2), (11); perturbation calculations (9), (18); and quantum statistical treatments (10). Reference (18) deals with the cooling of both free and bound atoms, and considers particularly the case of a harmonically bound atom. References (9), (10) and (11) deal specifically with harmonically trapped ions.

The treatments of (9), (10), (11) and (18) have been applied to an ion in a radio frequency quadrupole trap. It was assumed that this was justified because classically a particle in a rapidly oscillating potential field, $\nu(R)\cos\Omega t$, can be considered to move as if acted on by a time independent effective potential, $\nabla\nu\cdot\nabla\nu/4M\Omega^2$ (12:90-93). A fully quantum mechanical justification of this assumption has recently been

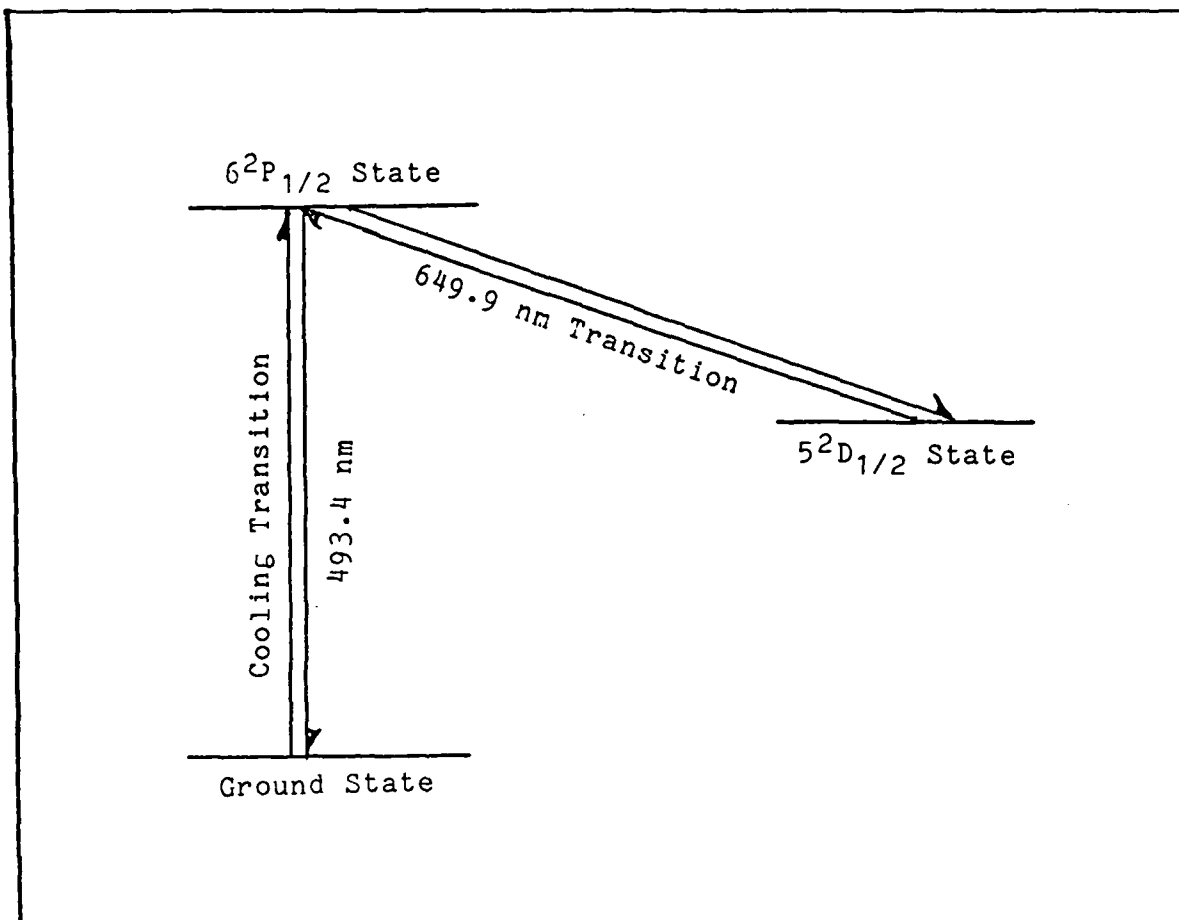


Figure 2. Energy level diagram for laser cooling arrangements.

given (4) and will be followed in Section II of this thesis for ion motion in the absence of laser cooling.

Reference (11) is the most detailed analysis of the final stages of the laser cooling process in a harmonic trap, and the density matrix equations derived here will be compared to the density matrix equations used there.

II. Ion Motion in the Absence of Laser Cooling

Effective Potential Solution

Cook et al. have developed the theory of particle motion in a rapidly oscillating field in Reference (4). That treatment will be followed here for the particular case of an ion in a radio frequency quadrupole trap.

In the absence of laser cooling, the forces acting on the ion in the trap are due entirely to the rf electric field. The electric potential for this field is given by equation (1). Schrodinger's equation for the particle's wave function in this case is

$$i\hbar \frac{\partial \psi}{\partial t} = -\frac{\hbar^2}{2M} \nabla^2 \psi + e v(\vec{R}) \cos \Omega t \psi \quad (2)$$

To understand the dominant effect of the potential, consider the solution to equation (2) if only the potential term is kept. The solution to the equation is then

$$\psi(\vec{R}, t) = \psi(\vec{R}, 0) \exp \left\{ -i \frac{\sin \Omega t}{\hbar \Omega} e v(R) \right\} = \psi(\vec{R}, 0) \Theta(\vec{R}, t) \quad (3)$$

Therefore, the principal effect of the electric field is an oscillating phase factor, Θ . A solution of the form

$$\Psi(\vec{R}, t) = \varphi(\vec{R}, t) \Theta(\vec{R}, t) \quad (4)$$

is assumed. The advantage of switching to φ is that φ is a slowly varying function of time compared to the rf field (4). The equation for φ is then

$$i\hbar \frac{\partial \varphi}{\partial t} = -\frac{\hbar^2}{2M} \nabla^2 \varphi + i \frac{e\hbar}{M\Omega} \sin \Omega t \nabla \varphi \cdot \vec{\nabla} v + 2 \frac{e^2 V_0^2}{M\Omega^2} (\chi^2 + Y^2 + 4Z^2) \sin^2 \Omega t \varphi \quad (5)$$

Substituting $\frac{1}{2}(1 - \cos 2\Omega t)$ for $\sin^2 \Omega t$ and making the rotating wave approximation of setting the rapidly oscillating terms, $\sin \Omega t$ and $\cos 2\Omega t$, to zero yields

$$i\hbar \frac{\partial \varphi}{\partial t} = -\frac{\hbar^2}{2M} \nabla^2 \varphi + \frac{e^2 V_0^2}{M\Omega^2} (\chi^2 + Y^2 + 4Z^2) \varphi \quad (6)$$

Equation (6) is the wave equation for an anisotropic harmonic oscillator with characteristic frequency $\nu = \frac{\sqrt{2} e V_0}{M\Omega}$ in the χ and Y directions and twice that in the Z direction. The total wave function is given by

$$\Psi_{ijk}(\vec{R}, t) = \psi_{ijk}(\vec{R}) e^{-iE_{ijk}t/\hbar} \Theta(\vec{R}, t) \quad (7)$$

where ψ_{ijk} is an appropriate harmonic oscillator wave function.

The matrix elements of the Hamiltonian in equation (2) between the wave functions of equation (7) are

$$\begin{aligned} H_{nn'} &= \langle \psi_n | \hat{H} | \psi_{n'} \rangle \\ &= \int d^3R \psi_n^* \Theta^* \left(-\frac{\hbar^2}{2M} \nabla^2 + eV(\vec{R}) \cos \Omega t \right) \psi_{n'} \Theta \end{aligned} \quad (8)$$

Applying the Laplacian operator yields

$$\begin{aligned} H_{nn'} &= \int d^3R \psi_n^* \left[-\frac{\hbar^2}{2M} \nabla^2 \psi_{n'} - \frac{e}{M\Omega} \sin \Omega t \vec{\nabla} \cdot \hat{p} \psi_{n'} \right. \\ &\quad \left. + 2 \frac{e^2 V_0^2}{M\Omega^2} \sin^2 \Omega t (\chi^2 + \gamma^2 + 4Z^2) \psi_{n'} \right. \\ &\quad \left. + eV_0 \cos \Omega t (\chi^2 + \gamma^2 - 2Z^2) \psi_{n'} \right] \end{aligned} \quad (9)$$

Substituting $\frac{1}{2}(1 - \cos 2\Omega t)$ for $\sin^2 \Omega t$ gives

$$\begin{aligned} H_{nn'} &= \int d^3R \psi_n^* \left[-\frac{\hbar^2}{2M} \nabla^2 \psi_{n'} + \frac{e^2 V_0^2}{M\Omega^2} (\chi^2 + \gamma^2 + 4Z^2) \psi_{n'} \right] \\ &\quad + \int d^3R \psi_n^* \left[-\frac{e}{M\Omega} \sin \Omega t \vec{\nabla} \cdot \hat{p} \psi_{n'} \right. \\ &\quad \left. - \frac{e^2 V_0^2}{M\Omega^2} \cos 2\Omega t (\chi^2 + \gamma^2 + 4Z^2) \psi_{n'} \right. \\ &\quad \left. + eV_0 \cos \Omega t (\chi^2 + \gamma^2 - 2Z^2) \psi_{n'} \right] \end{aligned} \quad (10)$$

The first group of bracketed terms is just $\delta_{nn'} E_n$. If only motion along the χ -axis is considered, equation (10) becomes

$$\begin{aligned}
H_{nn'} = & \delta_{nn'} \left[E_n + E_n \frac{\hbar}{2\sqrt{M}} \left(eV_0 \cos \Omega t + \frac{e^2 V_0^2}{M \Omega^2} \cos 2\Omega t \right) \right. \\
& \left. - \frac{i e V_0 \sqrt{\hbar}}{M \Omega \sqrt{2\sqrt{M}}} \sin \Omega t \right] \\
+ & \delta_{nn-2} \sqrt{n' / (n'-1)} \left[\frac{\hbar}{2\sqrt{M}} \left(eV_0 \cos \Omega t - \frac{e^2 V_0^2}{M \Omega^2} \cos 2\Omega t \right) \right. \\
& \left. + i \frac{e V_0 \sqrt{\hbar}}{M \Omega \sqrt{2\sqrt{M}}} \sin \Omega t \right] \\
+ & \delta_{nn+2} \sqrt{(n+1) / n} \left[\frac{\hbar}{2\sqrt{M}} \left(eV_0 \cos \Omega t - \frac{e^2 V_0^2}{M \Omega^2} \cos 2\Omega t \right) \right. \\
& \left. - i \frac{e V_0 \sqrt{\hbar}}{M \Omega \sqrt{2\sqrt{M}}} \sin \Omega t \right]
\end{aligned} \tag{11}$$

There are allowed transitions between the n and $n \pm 2$ levels, with transition frequency 2ν . The terms which drive these transitions have frequencies Ω and 2Ω . A resonant frequency, Ω_0 is defined as $\Omega_0^2 = \sqrt{2} eV_0 / M$. When $\Omega = \Omega_0$ or $\Omega = \Omega_0 / \sqrt{2}$, one of the driving frequencies equals the transition frequency, 2ν , and strong transitions are expected. Actually, it is shown in Reference (4) that for any positive integer r , Ω_0 / \sqrt{r} is a resonance frequency and strong transitions occur. Thus, stable trapping should occur only for values of Ω larger than Ω_0 . For the parameters of the experiment of References (16) and (15), $\Omega = 1.9 \Omega_0$. The trapping stability of these parameters will be examined for the wave packet solution.

The results so far derived differ from the effective potential solution assumed in Reference (11) in two respects. First, the phase factor, Θ , does not appear at all in the solution assumed in Reference (11). Second, the harmonic oscillator wave functions of Reference (11) are considered to be stationary states in the absence of laser cooling, and,

obviously, the wave functions of equation (7) are not. The effect of the phase factor on the laser cooling process will be discussed in Section III.

Wave Packet Solution

For one dimensional motion, a wave packet solution to equation (2) is

$$\psi(x,t) = \exp\left\{-\frac{M\omega}{2\hbar}(x-q)^2 + \frac{i}{\hbar}P\chi - \frac{i}{\hbar}\beta\right\} \quad (12)$$

where M is the mass of the ion, $q(t)$ and $P(t)$ are real and correspond to $\langle \hat{x} \rangle$ and $\langle \hat{p} \rangle$, and $\omega(t)$ and $\beta(t)$ are complex. The importance of ω is that the width of the packet, w , equals $\sqrt{\hbar/M \operatorname{Re}(\omega)}$. β represents normalization of ψ and phase. Substituting equation (12) into equation (2), equating coefficients of powers of χ , and assuming that $\dot{q} = P/M$ yields

$$\dot{P} = -2eV_0 q \cos \Omega t \quad (13a)$$

$$i\dot{\omega} = \omega^2 - \frac{2eV_0}{M} \cos \Omega t \quad (13b)$$

$$\dot{\beta} = \frac{1}{2}\hbar\omega + \frac{P^2}{2M} - 2eV_0 q^2 \cos \Omega t \quad (13c)$$

The equations for \dot{q} and \dot{p} mean that the particle moves classically, that is $d\langle\hat{x}\rangle/dt = \langle\hat{p}\rangle/m$ and $d\langle\hat{p}\rangle/dt = \langle F \rangle$, where F is the force.

The quantity of interest is ω . The equation for ω is a generalized Riccati equation (14:20-23). This equation can only be solved analytically when all the terms are polynomials. If the substitutions $\omega = -i\dot{m}/m$ and $\tau = \Omega t/2$ are made equation (13b) becomes

$$\frac{d^2 m}{d\tau^2} = \left[-2 \left(\frac{4eV_0}{M\Omega} \right) \cos 2\tau \right] m \quad (14)$$

This is Mathieu's equation. Much is known about the solutions to Mathieu's equation, Mathieu functions, but they can only be represented by simple functions in special cases (1:721-750). The general form of Mathieu's equation is

$$m'' = (a - 2q \cos 2\tau) m \quad (15)$$

For the values of V_0 and Ω used in the experiment of References (15) and (16) $a=0$ and $q=0.377$. The solution of equation (15) for these values of a and q is in what is known as a stable region. In this region the modulus of the Mathieu function is always finite for finite times. For $\Omega = \Omega_0$, $a=0$ and $q=1.41$. The solution of equation (12) for these values is

in an unstable region. In this region the modulus of the Mathieu function becomes infinite, on a finite interval, at least once (1:728). If $m = a + ib$ then the width of the wave packet is given by

$$W = \sqrt{\frac{\hbar(a^2 + b^2)}{M(ab' - a'b)}} \quad (16)$$

The modulus of the Mathieu function is $\sqrt{a^2 + b^2}$, so the numerator of equation (16) will become infinite at least once in a finite time for $\Omega = \Omega_0$. This does not necessarily mean that the width becomes infinite, which corresponds to the ion escaping, because the denominator might also become infinite. To understand more about the behavior of the width of the wave function it is necessary to examine equation (13b) numerically.

Returning to equation (13b), if $w = y + iz$, $\tau = vt$, $f = \Omega/v$, and $k = 2eV_0/Mv$ then

$$\frac{dy}{d\tau} = \frac{1}{v} 2yz \quad (17a)$$

$$\frac{dz}{d\tau} = k \cos f\tau + \frac{1}{v}(z^2 - y^2) \quad (17b)$$

Equations (17) were integrated numerically by a Runge-Kutta method (8:212). The calculation was done on a Columbia Model 1600 Personal Computer using the Basic language. The text of the program is in the Appendix. Three sets of values for the

constants were used; the values from the experiment of References (15) and (16) where $\Omega = 1.9\Omega_0$, values for $\Omega = 10\Omega_0$ and values for $\Omega = \Omega_0$.

Figure 3 is a plot of the width of the wave packet versus time for the values of V_0 and Ω used in the experiments of References (15) and (16). The initial width was taken to be the width of the ground state harmonic oscillator wave function, $w_0 = \sqrt{\hbar/MV}$. The width oscillates. The oscillation is actually two superimposed oscillations with frequencies Ω and $2V$. The width stays within 3 nm of the original value. From an initial value of 5.54 nm, it reaches a maximum value of 8.28 nm and a minimum value of 3.73 nm. The width of the second excited state (first allowed transition) of the harmonic oscillator wave function is given by $\sqrt{5} w_0$. For this case that would be 12.4 nm, so it is obvious that the ion is not being excited to higher levels and is stably trapped.

Figure 4 is a plot the width of the wave packet versus time for the value of V_0 used in the experiment and $\Omega = 10\Omega_0$. The initial value of the width was again taken to be the width of the ground state harmonic oscillator wave function, in this case 12.6 nm. The width again oscillates with two frequencies, Ω and $2V$. The variation from the initial value of the width in this case is much less than the variation for $\Omega = 1.9\Omega_0$.

Figure 5 is a plot of the width of the wave packet versus time for the value of V_0 used in the experiment and $\Omega = \Omega_0$. The initial value of the width was again taken to be the width of

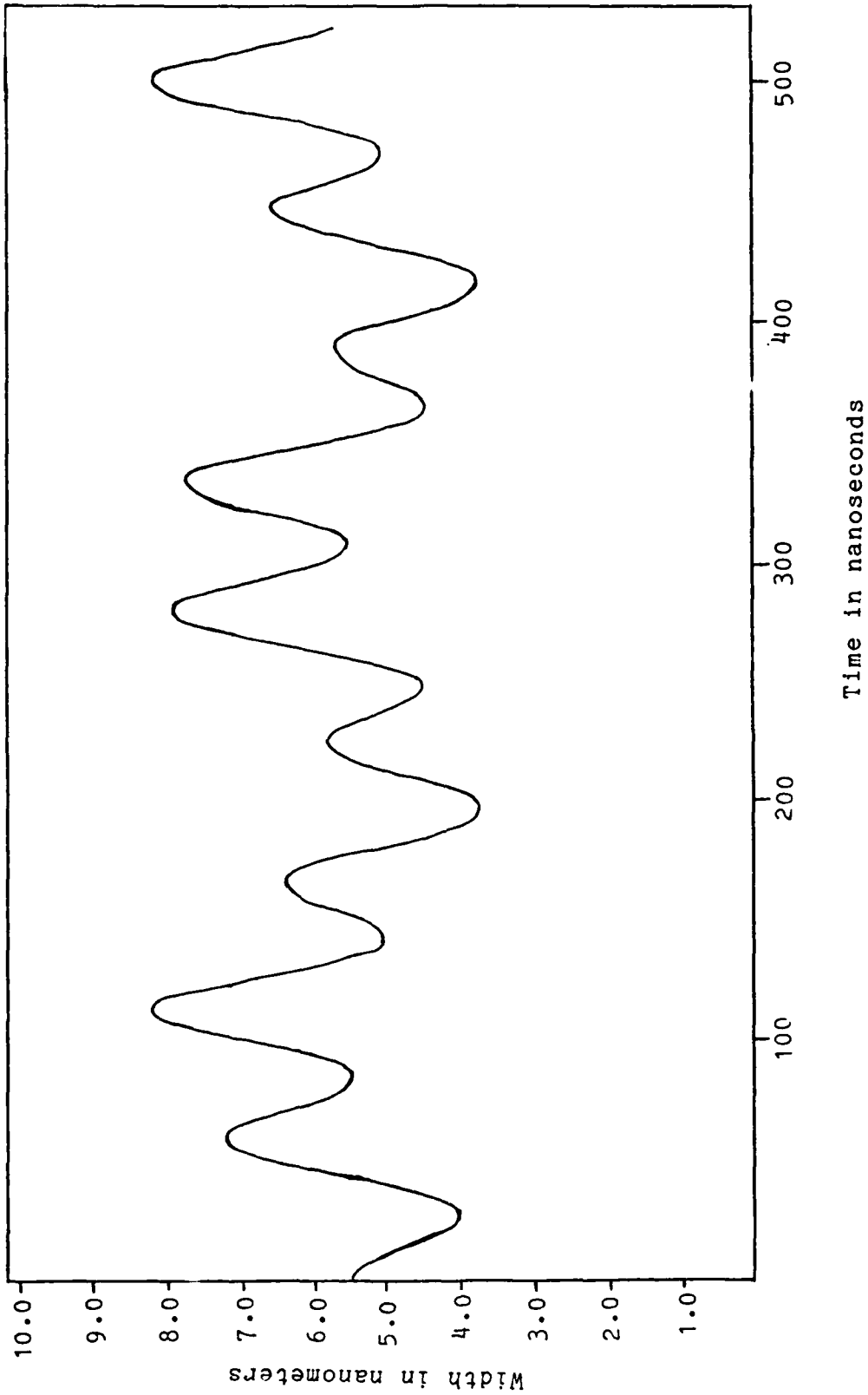


Figure 3. Graph of width versus time for the parameters used in the experiment.

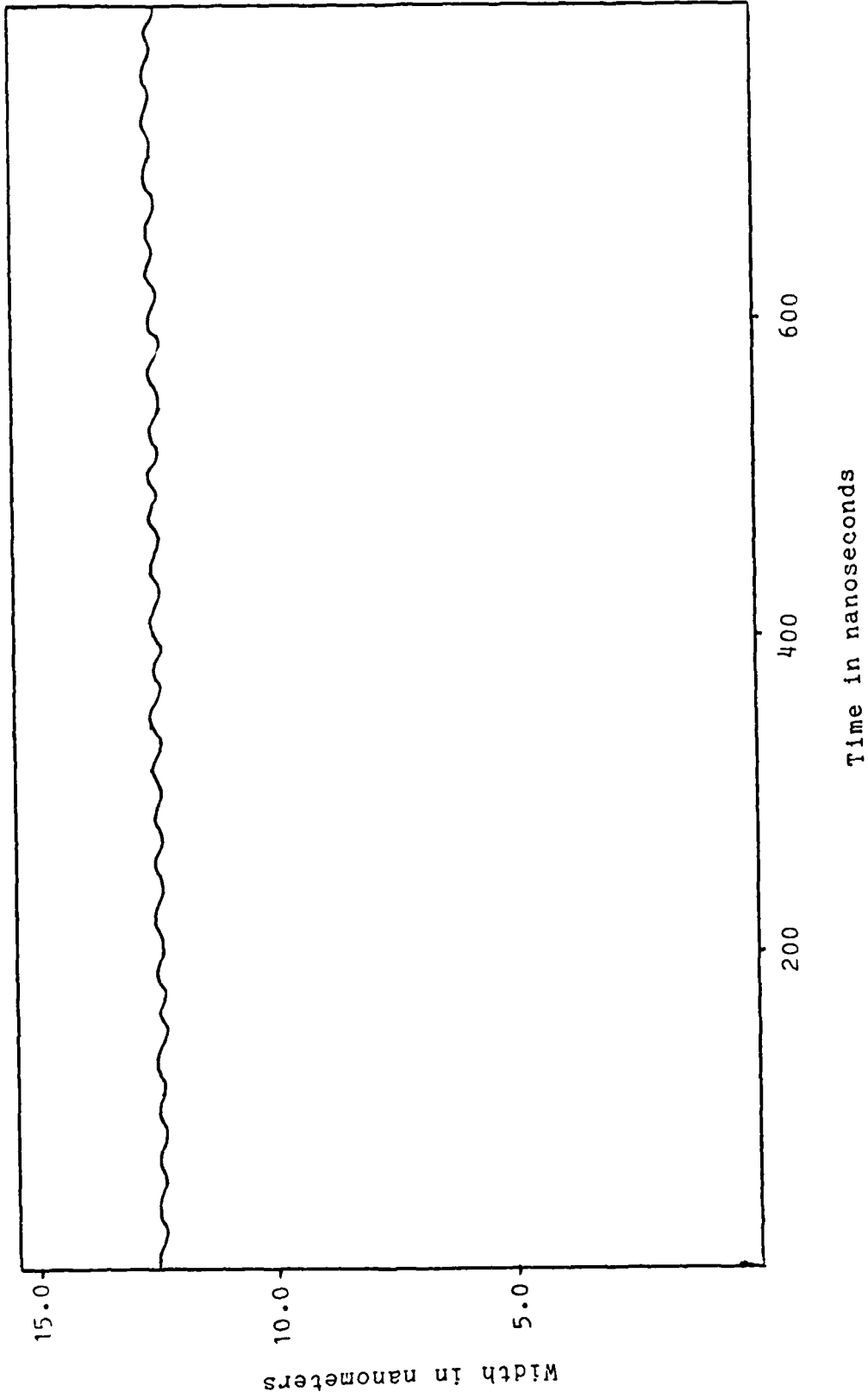
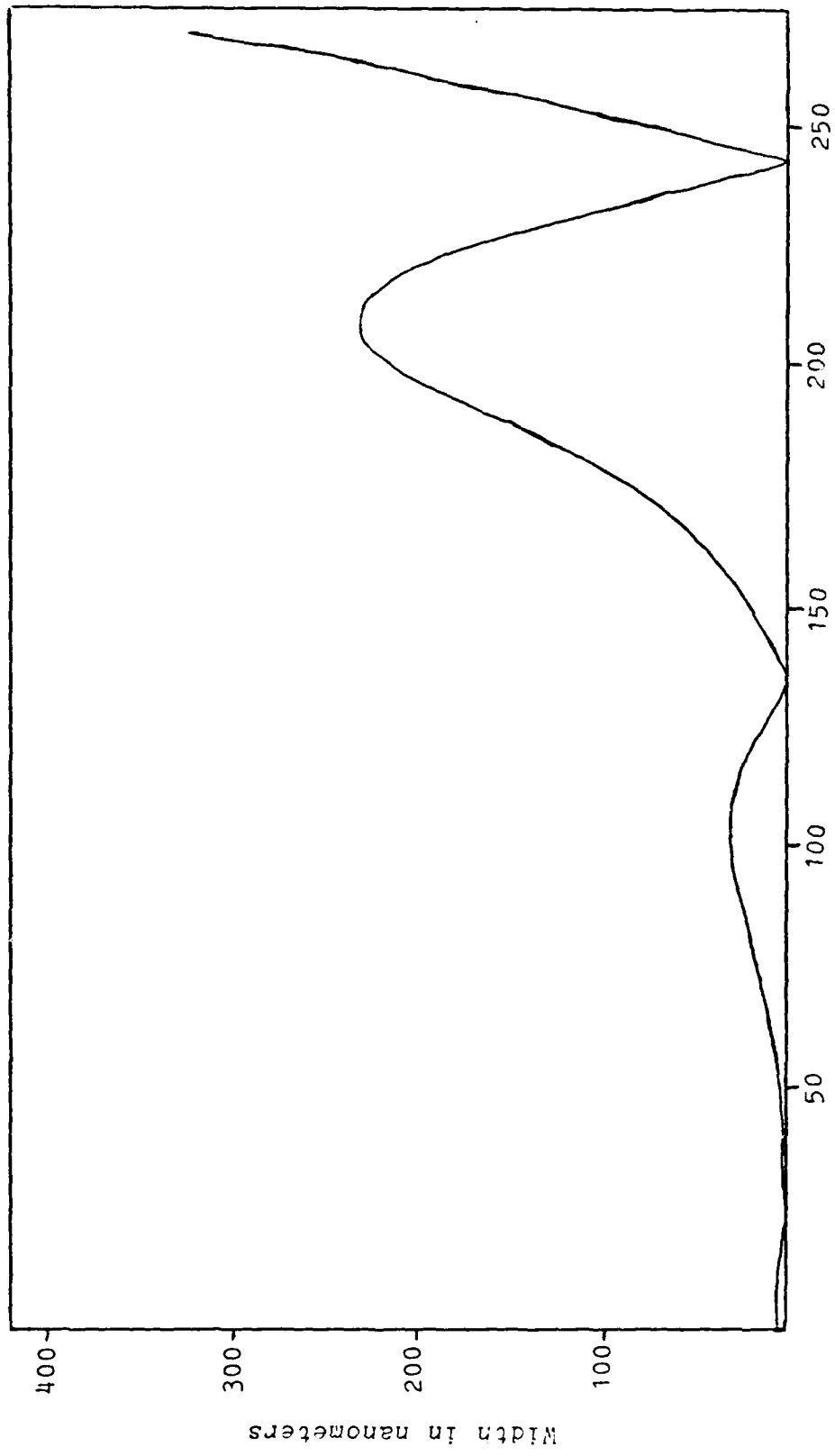


Figure 4. Graph of width versus time for $\Omega = 10\Omega_0$.



Time in nanoseconds

Figure 5. Graph of width versus time for $\Omega = \Omega_0$.

the ground state harmonic oscillator wave function, for this case 3.98 nm. The minimums and maximums for this case occur at regular intervals. The spacing from minimum to minimum and maximum to maximum is about 210 ns. Each maximum is about 145 ns from the minimum preceeding it and about 65 ns from the minimum following it. There is a maximum of 1702 nm at 611 ns, which is past the end of the plot. There should be a minimum at about 656 ns. The value at this minimum could not be calculated. The program calculates the values of γ and Z from equations (14). The width, W , is $\sqrt{F_{VM} \gamma}$, so that a minimum in W is a maximum for γ . When the program approaches the maximum in at 656 ns, the value calculated for γ overflows its register. This corresponds to a value for the width of the wave packet that is less than 10^{-20} cm. This is an unreasonably small value for the width, so the overflow is probably due to an instability in the integration technique. However, when the time step is cut in half, the value for γ overflows at the same point in time. A further examination of the width for this case could be done, however, it seems probable that the particle is undergoing strong transitions for the chosen values of V_0 and Ω , and the trend in the width for each successive maximum to be larger than the one preceeding it indicates that the particle will escape.

III. The Laser Cooling Process

Hamiltonian Matrix Elements

The ion in the trap is considered to be a two level system as regards electronic transitions for this section of the thesis. The basis states of the complete system are

$$\psi_{nm} = \psi_n(\vec{R}) e^{-iE_n t/\hbar} \Theta(\vec{R}, t) \phi_m(\vec{r}) e^{-iE_m t/\hbar} \quad (18)$$

where ϕ_m is the wave function for the electronic state with $m = 0, 1$, ψ_n is the wave function for the harmonic oscillator state with $n = 0, 1, 2, 3, \dots$, and Θ is the phase factor from equation (3). The energy of the system is the energy of the electronic state, $\hbar\omega_0 m$ plus the energy of the harmonic oscillator state, $\hbar\nu(n + 1/2)$. The energy level arrangement is shown in Figure 6.

The Hamiltonian for an ion in the trap in the presence of laser cooling can be divided into two parts, the Hamiltonian for the internal motion of the outer electron, \hat{H}_I , and the Hamiltonian for the translational motion of the ion in the trap, \hat{H}_E . Each of these can in turn be divided into two parts, the part that is present in the absence of the laser, \hat{H}_I^0 and \hat{H}_E^0 , and the part due to the laser, \hat{H}_I' and \hat{H}_E' . These are

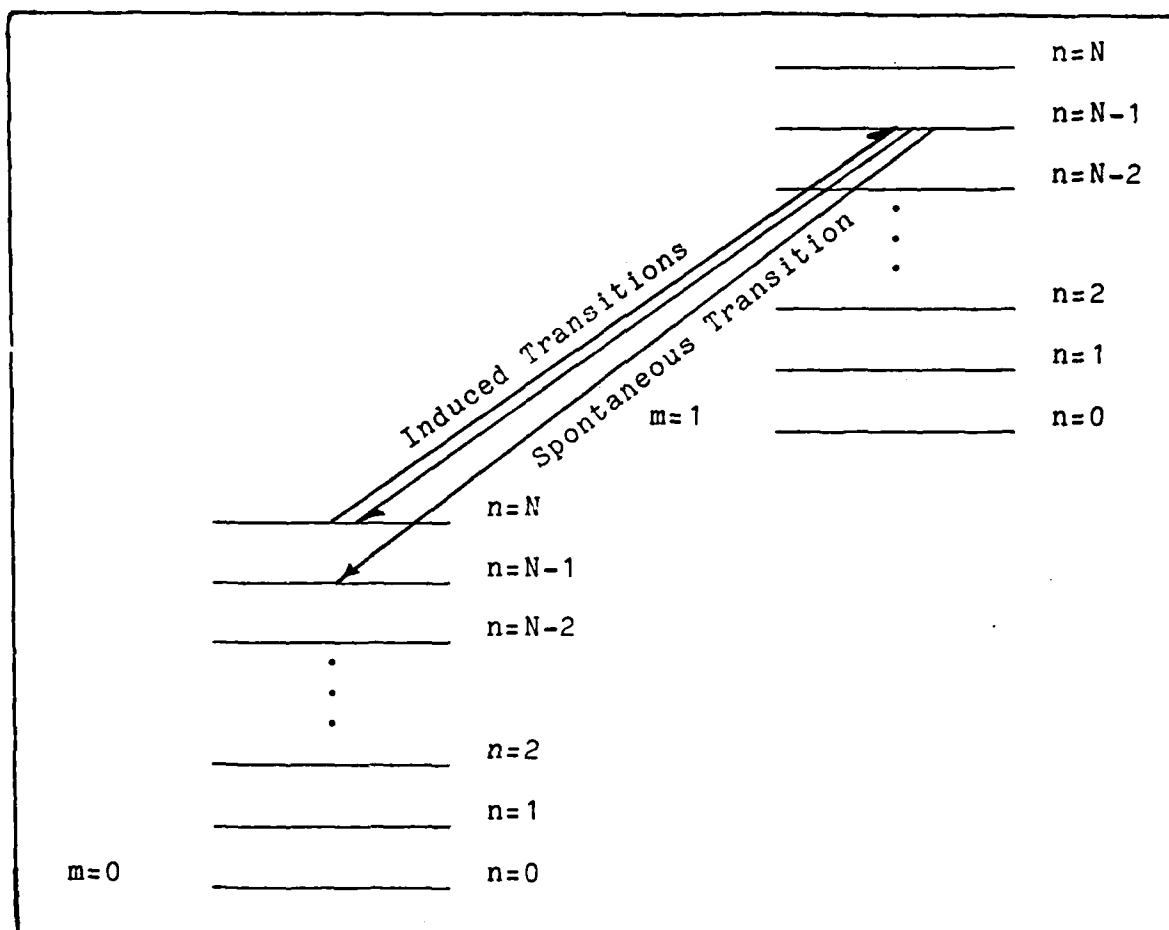


Figure 6. Energy levels and transitions of the ionic system in the quadropole trap. The electronic level is indexed by m , and the harmonic level is indexed by n .

$$\hat{H}_I^0 = \frac{\hat{p}^2}{2m} - \frac{2e^2}{r} \quad (19a)$$

$$\hat{H}_I' = -\vec{\mu}(\vec{r}) \cdot \vec{E}(\vec{R}, t) \quad (19b)$$

$$\hat{H}_E^0 = \frac{\hat{P}^2}{2M} + eV_0(\chi^2 + \gamma^2 - 2z^2) \cos \Omega t \quad (19c)$$

$$\hat{H}_E' = \frac{e}{2Mc} (\hat{P} \cdot \vec{A}(\vec{R}, t) + \vec{A}(\vec{R}, t) \cdot \hat{P}) \quad (19d)$$

where \hat{p} is the momentum operator corresponding to the outer electron's position with respect to the nucleus of the ion, \vec{r} , \hat{P} is the momentum operator corresponding to the ion's center of mass position in the trap, \vec{R} , m is the mass of the electron, M is the mass of the ion, \vec{E} is the electric field due to the laser, and \vec{A} is the vector potential due to the laser. In choosing \hat{H}_I' the dipole approximation has been made. At the center of the trap, the laser radiation can be approximated by a plane wave, so that \vec{E} and \vec{A} are

$$\vec{E} = \vec{E}_0 \cos(\vec{k} \cdot \vec{R} - \omega t) \quad (20)$$

$$\vec{A} = \frac{c}{\omega} \vec{E}_0 \sin(\vec{k} \cdot \vec{R} - \omega t) \quad (21)$$

The matrix elements for all the parts of the Hamiltonian of equations (19) with the wave functions of equation (18) can then be found. For \hat{H}_I^0 the matrix elements are

$$H_{I n m n' m'}^0 = \langle \psi_{nm} | \hat{H}_I^0 | \psi_{n'm'} \rangle = \delta_{nn'} \delta_{mm'} \hbar \omega_0 m \quad (22)$$

For \hat{H}'_I the matrix elements are

$$H'_{Inmn'm'} = - \left(\int d^3r \phi_m^* \vec{\mu}(\vec{r}) \phi_{m'} \right) \cdot \left(\int d^3R u_n^* \vec{E}(\vec{R}, t) u_{n'} \right) \quad (23)$$

Three simplifying assumptions can be made about $\vec{\mu}$: $\vec{\mu}$ is assumed to be real and given by $\vec{\mu} = \hat{u} e a_0$ where \hat{u} is a unit vector, e is the electronic charge, and a_0 is the Bohr radius; $\vec{E}_0 \cdot \vec{\mu} = E_0 \mu$; and a two by two matrix, $\mu_{mm'}$, defined below can be used to represent the integral of $\phi_m^* \mu \phi_{m'}$ over d^3r .

$$\mu_{mm'} = \mu \delta_{mm'} = \mu \begin{pmatrix} 0 & 1 \\ 1 & 0 \end{pmatrix} \quad (24)$$

Then the matrix elements of \hat{H}'_I can be written as

$$H'_{Inmn'm'} = - E_0 \mu_{mm'} \int d^3R u_n^* \cos(\vec{k} \cdot \vec{R} - \omega t) u_{n'} \quad (25)$$

In the Lambe-Dicke limit $\vec{k} \cdot \vec{R}$ is much less than unity and

$$\cos(\vec{k} \cdot \vec{R} - \omega t) = \cos \omega t + \vec{k} \cdot \vec{R} \sin \omega t \quad (26)$$

so that $H'_{Inmn'm'}$ becomes

$$H'_{I n m n' m'} = -E_0 \mu_{m m'} \delta_{n n'} \cos \omega t + E_0 \mu_{m m'} \sin \omega t \vec{k} \cdot \int d^3 R u_n^* \vec{R} u_{n'} \quad (27)$$

For one dimensional motion of the center of mass along the x -axis, this is

$$H'_{I n m n' m'} = -E_0 \mu_{m m'} \delta_{n n'} \cos \omega t - E_0 \mu_{m m'} k_x \sqrt{\frac{\hbar}{2M}} \sin \omega t \times (\sqrt{n'} \delta_{n n'-1} + \sqrt{n} \delta_{n n'+1}) \quad (28)$$

The matrix elements of \hat{H}_E^0 are

$$H_{E n m n' m'}^0 = \delta_{m m'} \int d^3 R u_n^* \Theta^* \left[-\frac{\hbar^2}{2M} \nabla^2 + v(\vec{R}) \cos \Omega t \right] u_{n'} \Theta \quad (29)$$

Applying the Laplacian operator yields

$$H_{E n m n' m'}^0 = \delta_{m m'} \int d^3 R u_n^* \left[-\frac{\hbar^2}{2M} \nabla^2 u_{n'} + \frac{2e^2 V_0^2}{M \Omega^2} \sin^2 \Omega t (x^2 + y^2 + 4z^2) u_{n'} + \frac{2eV_0}{M \Omega} \sin \Omega t (x \hat{i} + y \hat{j} - 2z \hat{k}) \cdot i \hbar \vec{\nabla} u_{n'} + eV_0 \cos \Omega t (x^2 + y^2 - 2z^2) u_{n'} \right] \quad (30)$$

Substituting $\frac{1}{2}(1 - \cos 2\Omega t)$ for $\sin^2 \Omega t$

$$\begin{aligned}
H_E^{\circ} n m n' m' &= \delta_{m m'} \delta_{n n'} E_n \\
&+ \delta_{m m'} \int d^3 R u_n^* \left[\frac{2eV_0}{M\Omega} \sin \Omega t (\chi \hat{i} + \gamma \hat{j} - 2Z \hat{k}) \cdot \hbar \nabla u_n \right. \\
&- \frac{e^2 V_0^2}{M\Omega^2} \cos 2\Omega t (\chi^2 + \gamma^2 + 4Z^2) u_n \\
&\left. + eV_0 \cos \Omega t (\chi^2 + \gamma^2 - 2Z^2) u_n \right]
\end{aligned} \tag{31}$$

For one dimensional motion of the center of mass along the χ - axis, this is

$$\begin{aligned}
H_E^{\circ} n m n' m' &= \delta_{m m'} \left\{ \delta_{n n'} \left[E_n + E_n \frac{\hbar}{2\mu M} (eV_0 \cos \Omega t + \frac{e^2 V_0^2}{M\Omega^2} \cos 2\Omega t) \right. \right. \\
&\quad \left. \left. - i \frac{eV_0}{M\Omega} \sqrt{\frac{\hbar}{\mu M}} \sin \Omega t \right] \right. \\
&+ \delta_{n n' \pm 2} \sqrt{n' \sqrt{n' \mp 1}} \left[\frac{\hbar}{2\mu M} (eV_0 \cos \Omega t - \frac{e^2 V_0^2}{M\Omega^2} \cos 2\Omega t) \right. \\
&\quad \left. + i \frac{eV_0}{M\Omega} \sqrt{\frac{\hbar}{\mu M}} \sin \Omega t \right] \\
&+ \delta_{n n' \pm 2} \sqrt{n' \sqrt{n' \mp 1}} \left[\frac{\hbar}{2\mu M} (eV_0 \cos \Omega t - \frac{e^2 V_0^2}{M\Omega^2} \cos 2\Omega t) \right. \\
&\quad \left. - i \frac{eV_0}{M\Omega} \sqrt{\frac{\hbar}{\mu M}} \sin \Omega t \right] \left. \right\}
\end{aligned} \tag{32}$$

It was shown in Section II of this thesis that in stable trapping situations strong transitions between the n and $n \pm 2$ levels do not occur. It will be assumed for simplicity that no transitions occur. When the terms involving transitions can be neglected, all other terms involving $\cos \Omega t$, $\sin \Omega t$, and $\cos 2\Omega t$ can be neglected also, so that $H_E^{\circ} n m n' m'$ can be approximated as

$$H_E^{\circ}{}_{nmn'm'} = \delta_{mm'} \delta_{nn'} E_n \quad (33)$$

The matrix elements for \hat{H}_E' are

$$H'_{Enmn'm'} = \delta_{mm'} \left(\frac{-i\hbar e}{2M\omega} \right) \vec{E}_0 \cdot \int d^3R u_n^* \Theta^* \times \left\{ \vec{\nabla} [\sin(\vec{k} \cdot \vec{R} - \omega t) u_{n'} \Theta] + \sin(\vec{k} \cdot \vec{R} - \omega t) \nabla(u_{n'} \Theta) \right\} \quad (34)$$

Applying the gradient operator and noting that $\vec{k} \cdot \vec{E}_0 = 0$ this becomes

$$H'_{Enmn'm'} = \delta_{mm'} \left(\frac{-i\hbar e}{M\omega} \right) \vec{E}_0 \cdot \int d^3R u_n^* \sin(\vec{k} \cdot \vec{R} - \omega t) \times [u_{n'} (2(X\hat{i} + Y\hat{j} - Z\hat{k})) + \vec{\nabla} u_{n'}] \quad (35)$$

In the Lamb-Dicke limit $\vec{k} \cdot \vec{R}$ is much less than unity, so that

$$\sin(\vec{k} \cdot \vec{R} - \omega t) = \vec{k} \cdot \vec{R} \cos \omega t - \sin \omega t \quad (36)$$

so that equation (35) becomes

$$H'_{Enmn'm'} = \delta_{mm'} \left(\frac{-i\hbar e}{M\omega} \right) \vec{E}_0 \cdot \left[-\sin \omega t \int d^3R u_n^* (u_{n'} \vec{\nabla} v + \vec{\nabla} u_{n'}) + \cos \omega t \int d^3R u_n^* (\vec{k} \cdot \vec{R}) (u_{n'} \vec{\nabla} v + \vec{\nabla} u_{n'}) \right] \quad (37)$$

This group of matrix elements cannot be as simply converted to one dimensional motion along the χ -axis, but this is unnecessary. The interaction between the ion and light field described by this part of the Hamiltonian is nonresonant. The cross-section for this interaction is the Thomas scattering cross-section, $\sigma_t = e^4 / 6\pi\epsilon_0^2 M^2 c^4$. For the intensity of light used in the experiment and a Ba^+ ion the rate for this interaction is on the order of 10^{-16} per second, which much less than the spontaneous emission rate of 1.9×10^7 . This part of the Hamiltonian can be neglected.

It can be seen from equations (32) and (37) that the phase factor, Θ , changes the matrix elements for \hat{H}_E^0 and \hat{H}_E' from what they would be if Θ were ignored. However, in all cases \hat{H}_E' can be neglected entirely, and in cases of stable trapping the terms in \hat{H}_E^0 $n m n' m'$ caused by Θ can be neglected. Thus, when considering laser cooling of a stably trapped ion, the effect of the phase factor can be neglected.

The matrix elements for the total Hamiltonian, $\hat{H} = \hat{H}_I^0 + \hat{H}_E^0 + \hat{H}_I'$ are

$$\begin{aligned}
 H_{n m n' m'} &= \delta_{m m'} \delta_{n n'} [\hbar \omega_0 m + \hbar \nu (n + 1/2)] \\
 &\quad - E_0 \mu_{m m'} \delta_{n n'} \cos \omega t \\
 &\quad E_0 \mu_{m m'} \sqrt{\frac{\hbar}{2 \nu M}} k_x \sin \omega t (\sqrt{n} \delta_{n n'-1} + \sqrt{n'} \delta_{n n'+1})
 \end{aligned}
 \tag{38}$$

There are induced transitions between the $m=0, n$ state and the $m=1, n$ or $n \pm 1$ state. If the laser is tuned below the resonance frequency to $\omega_0 - \nu$ then the induced transition between the $m=0, n$ state and the $m=1, n-1$ state will dominate.

Spontaneous emission has not been included in the Hamiltonian. The dominant spontaneous transition will be from the $m=1, n$ level to the $m=0, n$ level. Both the induced and spontaneous transitions are shown on the energy level diagram of Figure 6. It can be seen from the diagram that the net effect of the combination of the induced transitions, both up and down, and the spontaneous transition down will be a decrease in the harmonic oscillator quantum number, which corresponds to cooling.

It should be noted that if the ion is cooled to the ground state of the harmonic oscillator, the induced transitions will not be able to occur. In the experiment of References (15) and (16), the ion fluorescence due to the induced absorption and spontaneous emission can be observed visually. If the ion is cooled to the ground state, a lessening in the intensity of the light should be observed. The light will not disappear entirely unless the natural linewidth of the transition is much less than the harmonic oscillator energy level spacing. The natural linewidth of the transition used in the experiment is $2\pi \times 19$ MHz (5:11), while the energy spacing between the harmonic oscillator levels is $2\pi \times 2.4$ MHz. A dip in the fluorescence could be used

experimentally to determine if the ion has been cooled to the ground state. To find the rate of cooling, i.e. the rate of change of \bar{n} , and to determine the change in the fluorescence when the particle is in the ground state it is necessary to develop the density matrix equations.

Development of Density Matrix Equations

A density operator, $\hat{\rho}$, can be defined for any quantum system (17:199). The density matrix for a particular representation is $\rho_{ik} = \langle i | \hat{\rho} | k \rangle$. For the representation used here for the ion system this is

$$\rho_{nmn'm'} = \langle \psi_{nm} | \hat{\rho} | \psi_{n'm'} \rangle \quad (39)$$

The density matrix is useful to work with at this point because the probability P_{nm} that the system is in a state ψ_{nm} is ρ_{nmnm} . If the density matrix is known at any time, it can be found at later times by the relation

$$\dot{\rho}_{nmn'm'} = \frac{1}{i\hbar} \sum_j \sum_i (H_{nmij} \rho_{ijn'm'} - \rho_{nmij} H_{ijn'm'}) \quad (40)$$

The Hamiltonian matrix elements should be for the complete Hamiltonian, including spontaneous emission. To include

spontaneous emission explicitly in the Hamiltonian it is necessary to quantize the electromagnetic field. Spontaneous emission can be included in the density matrix equations by following the treatment of Reference (13). The density matrix equations including spontaneous emission terms are

for $m \neq m'$ or $n \neq n'$

$$\dot{\rho}_{nmn'm'} = \frac{1}{i\hbar} \sum_j \sum_i (H_{nmij} \rho_{ijn'm'} - \rho_{nmij} H_{ijn'm'}) - \frac{1}{2} \left(\sum_{j < m} \sum_i A_{nmij} + \sum_{j < m'} \sum_i A_{n'm'ij} \right) \rho_{nmn'm'} \quad (41a)$$

for $m = m'$ and $n = n'$

$$\dot{\rho}_{nmnm} = \frac{1}{i\hbar} \sum_j \sum_i (H_{nmij} \rho_{ijnm} - \rho_{nmij} H_{ijnm}) - \left(\sum_{j < m} \sum_i A_{nmij} \right) \rho_{nmnm} + \sum_{j > m} \sum_i A_{ijnm} \rho_{ijij} \quad (41b)$$

For the purposes of this thesis, spontaneous emission is assumed to occur only from the $m=1, n$ state to the $m=0, n$ state. This is a valid assumption if the natural linewidth of the transition is much less than the spacing of the harmonic oscillator energy levels. For this case,

$$A_{nmn'm'} = A \delta_{nn'} \beta_{mm'} = A \delta_{nn'} \begin{pmatrix} 0 & 0 \\ 1 & 0 \end{pmatrix} \quad (42)$$

A matrix, $\alpha_{nmn'm'}$ is defined as

$$\alpha_{nmn'm'} = \sum_j \sum_i (H_{nmij} \rho_{ijn'm'} - \rho_{nmij} H_{ijn'm'}) \quad (43)$$

Substituting the matrix elements of equation (38) into equation (43) and noting that

$$\sum_i \delta_{n,i+1} \sqrt{n} \rho_{i,j n' m'} = \sqrt{n} \rho_{(n-1),j n' m'} \quad (44a)$$

$$\sum_i \delta_{n,i-1} \sqrt{i} \rho_{i,j n' m'} = \sqrt{n+1} \rho_{(n+1),j n' m'} \quad (44b)$$

$$\sum_i \delta_{i n'+1} \sqrt{i} \rho_{n m i j} = \sqrt{n'+1} \rho_{n m (n'+1) j} \quad (44c)$$

$$\sum_i \delta_{i n'-1} \sqrt{n'} \rho_{n m i j} = \sqrt{n'} \rho_{n m (n'-1) j} \quad (44d)$$

yields

$$\begin{aligned} \alpha_{n m n' m'} &= [\hbar \omega (m - m') + \hbar \nu (n - n')] \rho_{n m n' m'} \\ &\quad - \mu E_0 \cos \omega t \sum_j (\delta_{m j} \rho_{n j n' m'} - \delta_{j m} \rho_{n m n' j}) \\ &\quad - \mu E_0 k_x \frac{\sqrt{\hbar}}{\sqrt{2 \nu M}} \sin \omega t \sum_j [(\sqrt{n} \rho_{(n-1) j n' m'} + \sqrt{n+1} \rho_{(n+1) j n' m'}) \delta_{m j} \\ &\quad \quad - (\sqrt{n'} \rho_{n m (n'-1) j} + \sqrt{n'+1} \rho_{n m (n'+1) j}) \delta_{j m'}] \end{aligned} \quad (45)$$

For given values of m and m' the sums over j can be performed.

$$\begin{aligned} \alpha_{n 0 n' 0} &= \hbar \nu (n - n') \rho_{n 0 n' 0} \\ &\quad - \mu E_0 \cos \omega t (\rho_{n 1 n' 0} - \rho_{n 0 n' 1}) \\ &\quad - \mu E_0 k_x \frac{\sqrt{\hbar}}{\sqrt{2 \nu M}} \sin \omega t [(\sqrt{n} \rho_{(n-1) 1 n' 0} + \sqrt{n+1} \rho_{(n+1) 1 n' 0}) \\ &\quad \quad - (\sqrt{n'} \rho_{n 0 (n'-1) 1} + \sqrt{n'+1} \rho_{n 0 (n'+1) 1})] \end{aligned} \quad (46a)$$

$$\begin{aligned}
\dot{\alpha}_{n0n'1} = & [-\hbar\omega_0 + \hbar\nu(n-n')] \rho_{n0n'1} \\
& - \mu E_0 \cos\omega t (\rho_{n1n'1} - \rho_{n0n'0}) \\
& - \mu E_0 k_x \sqrt{\frac{\hbar}{2\nu m}} \sin\omega t \left[\sqrt{n} \rho_{(n-1)n'1} + \sqrt{n+1} \rho_{(n+1)n'1} \right. \\
& \quad \left. - (\sqrt{n'} \rho_{n0(n'-1)0} + \sqrt{n'+1} \rho_{n0(n'+1)0}) \right]
\end{aligned} \tag{46b}$$

$$\begin{aligned}
\dot{\alpha}_{n1n'0} = & [\hbar\omega_0 + \hbar\nu(n-n')] \rho_{n1n'0} \\
& - \mu E_0 \cos\omega t (\rho_{n0n'0} - \rho_{n1n'1}) \\
& - \mu E_0 k_x \sqrt{\frac{\hbar}{2\nu m}} \sin\omega t \left[(\sqrt{n} \rho_{(n-1)n'0} + \sqrt{n+1} \rho_{(n+1)n'0}) \right. \\
& \quad \left. - (\sqrt{n'} \rho_{n1(n'-1)1} + \sqrt{n'+1} \rho_{n1(n'+1)1}) \right]
\end{aligned} \tag{46c}$$

$$\begin{aligned}
\dot{\alpha}_{n1n'1} = & \hbar\nu(n-n') \rho_{n1n'1} \\
& - \mu E_0 \cos\omega t (\rho_{n0n'1} - \rho_{n1n'0}) \\
& - \mu E_0 k_x \sqrt{\frac{\hbar}{2\nu m}} \sin\omega t \left[(\sqrt{n} \rho_{(n-1)n'1} + \sqrt{n+1} \rho_{(n+1)n'1}) \right. \\
& \quad \left. - (\sqrt{n'} \rho_{n1(n'-1)0} + \sqrt{n'+1} \rho_{n1(n'+1)0}) \right]
\end{aligned} \tag{46d}$$

Noting that

$$\sum_{j < n} \sum_i A_{nmi} \dot{\alpha}_{ij} = A \begin{cases} 0 & m=0 \\ 1 & m=1 \end{cases} \tag{47a}$$

$$\sum_{j > m} \sum_i A_{ijnm} \dot{\alpha}_{ij} = A \begin{cases} \rho_{n1n1} & m=0 \\ 0 & m=1 \end{cases} \tag{47b}$$

the density matrix equations can be written as

$$\begin{aligned} \dot{\rho}_{n_0 n'_0} = & \sum_{n''} A \rho_{n'' n'_1} + i\nu(n'-n)\rho_{n_0 n'_0} \\ & + i\frac{\mu E_0}{\hbar} \cos \omega t (\rho_{n_1 n'_0} - \rho_{n_0 n'_1}) \\ & + i\frac{\mu E_0}{\hbar} k_x \sqrt{\frac{\hbar}{2\nu M}} \sin \omega t \left[(\sqrt{n} \rho_{(n-1)n'_0} + \sqrt{n+1} \rho_{(n+1)n'_0}) \right. \\ & \left. - (\sqrt{n'} \rho_{n_0(n'-1)_1} + \sqrt{n'+1} \rho_{n_0(n'+1)_0}) \right] \end{aligned} \quad (48a)$$

$$\begin{aligned} \dot{\rho}_{n_0 n'_1} = & \left\{ i[\omega_0 + (n'-n)\nu] - \frac{A}{2} \right\} \rho_{n_0 n'_1} \\ & + i\frac{\mu E_0}{\hbar} \cos \omega t (\rho_{n_1 n'_1} - \rho_{n_0 n'_0}) \\ & + i\frac{\mu E_0}{\hbar} k_x \sqrt{\frac{\hbar}{2\nu M}} \sin \omega t \left[(\sqrt{n} \rho_{(n-1)n'_1} + \sqrt{n+1} \rho_{(n+1)n'_1}) \right. \\ & \left. - (\sqrt{n'} \rho_{n_1(n'-1)_1} + \sqrt{n'+1} \rho_{n_1(n'+1)_1}) \right] \end{aligned} \quad (48b)$$

$$\begin{aligned} \dot{\rho}_{n_1 n'_0} = & \left\{ i[\omega_0 + (n'-n)\nu] - \frac{A}{2} \right\} \rho_{n_1 n'_0} \\ & + i\frac{\mu E_0}{\hbar} \cos \omega t (\rho_{n_0 n'_0} - \rho_{n_1 n'_1}) \\ & + i\frac{\mu E_0}{\hbar} k_x \sqrt{\frac{\hbar}{2\nu M}} \sin \omega t \left[(\sqrt{n} \rho_{(n-1)n'_0} + \sqrt{n+1} \rho_{(n+1)n'_0}) \right. \\ & \left. - (\sqrt{n'} \rho_{n_1(n'-1)_1} + \sqrt{n'+1} \rho_{n_1(n'+1)_1}) \right] \end{aligned} \quad (48c)$$

$$\begin{aligned} \dot{\rho}_{n_1 n'_1} = & [i(n'-n)\nu - A] \rho_{n_1 n'_1} \\ & + i\frac{\mu E_0}{\hbar} \cos \omega t (\rho_{n_0 n'_1} - \rho_{n_1 n'_0}) \\ & + i\frac{\mu E_0}{\hbar} k_x \sqrt{\frac{\hbar}{2\nu M}} \sin \omega t \left[(\sqrt{n} \rho_{(n-1)n'_1} + \sqrt{n+1} \rho_{(n+1)n'_1}) \right. \\ & \left. - (\sqrt{n'} \rho_{n_1(n'-1)_0} + \sqrt{n'+1} \rho_{n_1(n'+1)_0}) \right] \end{aligned} \quad (48d)$$

The equations for the density matrix elements when $m \neq m'$ contain the resonant frequency for the transition, ω_0 . These elements will oscillate rapidly. A substitution can be made to change to a more slowly varying function, $\sigma_{nmn'm'}$. It is

$$\rho_{n_0 n'_0} = \sigma_{n_0 n'_0} \quad (49a)$$

$$\rho_{n_0 n'_1} = e^{i\omega t} \sigma_{n_0 n'_1} \quad (49b)$$

$$\rho_{n,n'0} = e^{-i\omega t} \sigma_{n,n'0} \quad (49c)$$

$$\rho_{n,n'1} = \sigma_{n,n'1} \quad (49d)$$

The equations for $\sigma_{nmn'm'}$ are

$$\begin{aligned} \dot{\sigma}_{non'0} = & \delta_{nn'} A \sigma_{n,n'1} + i(n'-n)\nu \sigma_{non'0} \\ & + i \frac{kE_0}{\hbar} \cos \omega t (e^{-i\omega t} \sigma_{n,n'0} - e^{i\omega t} \sigma_{non'1}) \\ & + i \frac{kE_0}{\hbar} k_x \sqrt{\frac{\hbar}{2\nu M}} \sin \omega t \left[e^{i\omega t} (\sqrt{n} \sigma_{(n-1)n'0} + \sqrt{n+1} \sigma_{(n+1)n'0}) \right. \\ & \left. - e^{-i\omega t} (\sqrt{n'} \sigma_{no(n'-1)1} + \sqrt{n'+1} \sigma_{no(n'+1)1}) \right] \end{aligned} \quad (50a)$$

$$\begin{aligned} \dot{\sigma}_{non'1} = & \left\{ i[(\omega_0 - \omega) + (n'-n)\nu] - \frac{A}{2} \right\} \sigma_{non'1} \\ & + i \frac{kE_0}{\hbar} \cos \omega t e^{-i\omega t} (\sigma_{n,n'1} - \sigma_{non'0}) \\ & + i \frac{kE_0}{\hbar} k_x \sqrt{\frac{\hbar}{2\nu M}} \sin \omega t e^{-i\omega t} \left[(\sqrt{n} \sigma_{(n-1)n'1} + \sqrt{n+1} \sigma_{(n+1)n'1}) \right. \\ & \left. - (\sqrt{n'} \sigma_{no(n'-1)0} + \sqrt{n'+1} \sigma_{no(n'+1)0}) \right] \end{aligned} \quad (50b)$$

$$\begin{aligned} \dot{\sigma}_{n,n'0} = & \left\{ i[(\omega - \omega_0) + (n'-n)\nu] - \frac{A}{2} \right\} \sigma_{n,n'0} \\ & + i \frac{kE_0}{\hbar} \cos \omega t e^{i\omega t} (\sigma_{non'0} - \sigma_{n,n'1}) \\ & + i \frac{kE_0}{\hbar} k_x \sqrt{\frac{\hbar}{2\nu M}} \sin \omega t e^{i\omega t} \left[(\sqrt{n} \sigma_{(n-1)on'0} + \sqrt{n+1} \sigma_{(n+1)on'0}) \right. \\ & \left. - (\sqrt{n'} \sigma_{n_1(n'-1)1} + \sqrt{n'+1} \sigma_{n_1(n'+1)1}) \right] \end{aligned} \quad (50c)$$

$$\begin{aligned} \dot{\sigma}_{n,n'1} = & [i(n'-n)\nu - A] \sigma_{n,n'1} \\ & + i \frac{kE_0}{\hbar} \cos \omega t (e^{i\omega t} \sigma_{non'1} - e^{-i\omega t} \sigma_{n,n'0}) \\ & + i \frac{kE_0}{\hbar} k_x \sqrt{\frac{\hbar}{2\nu M}} \sin \omega t \left[e^{i\omega t} (\sqrt{n} \sigma_{(n-1)on'1} + \sqrt{n+1} \sigma_{(n+1)on'1}) \right. \\ & \left. - e^{-i\omega t} (\sqrt{n'} \sigma_{n_1(n'-1)0} + \sqrt{n'+1} \sigma_{n_1(n'+1)0}) \right] \end{aligned} \quad (50d)$$

If $\sin \omega t$ and $\cos \omega t$ are written in terms of exponentials it can be seen that

$$\cos \omega t e^{\pm i \omega t} = \frac{1}{2} (e^{i 2 \omega t} + e^0) \approx \frac{1}{2}$$

$$\sin \omega t e^{\pm i \omega t} = \pm \frac{1}{2} (e^0 - e^{i 2 \omega t}) \approx \pm \frac{1}{2} \quad (51b)$$

because $e^{i 2 \omega t}$ averages to zero over a very short time and can be disregarded. For cooling purposes the laser frequency, ω , is tuned below the resonant frequency of the transition, by an amount ν . So that the equations for the slowly varying parts of the density matrix are

$$\begin{aligned} \dot{\sigma}_{non'o} = & \delta_{nn'} A \sigma_{n|n'} + i \nu (n'-n) \sigma_{non'o} \\ & + i \frac{\mu E_0}{2 \hbar} (\sigma_{n|n'o} - \sigma_{non'n'}) \\ & + \frac{\mu E_0}{2 \hbar} k_x \sqrt{\frac{\hbar}{2 \nu M}} \left[\sqrt{n} \sigma_{(n-1)|n'o} + \sqrt{n+1} \sigma_{(n+1)|n'o} \right. \\ & \left. + \sqrt{n'} \sigma_{no(n'-1)|} + \sqrt{n'+1} \sigma_{no(n'+1)|} \right] \end{aligned} \quad (52a)$$

$$\begin{aligned} \dot{\sigma}_{non'n'} = & \left[i \nu (n'+1-n) - \frac{A}{2} \right] \sigma_{non'n'} \\ & + i \frac{\mu E_0}{2 \hbar} (\sigma_{n|n'n'} - \sigma_{non'n'o}) \\ & + \frac{\mu E_0}{2 \hbar} k_x \sqrt{\frac{\hbar}{2 \nu M}} \left[(\sqrt{n} \sigma_{(n-1)|n'n'} + \sqrt{n+1} \sigma_{(n+1)|n'n'}) \right. \\ & \left. - (\sqrt{n'} \sigma_{no(n'-1)o} + \sqrt{n'+1} \sigma_{no(n'+1)o}) \right] \end{aligned} \quad (52b)$$

$$\begin{aligned} \dot{\sigma}_{n|n'o} = & \left[i \nu (n'-1-n) - \frac{A}{2} \right] \sigma_{n|n'o} \\ & + i \frac{\mu E_0}{2 \hbar} (\sigma_{non'o} - \sigma_{n|n'n'}) \\ & + \frac{\mu E_0}{2 \hbar} k_x \sqrt{\frac{\hbar}{2 \nu M}} \left[(\sqrt{n'} \sigma_{n|(n'-1)|} + \sqrt{n'+1} \sigma_{n|(n'+1)|}) \right. \\ & \left. - (\sqrt{n} \sigma_{(n-1)|n'o} + \sqrt{n+1} \sigma_{(n+1)|n'o}) \right] \end{aligned} \quad (52c)$$

$$\begin{aligned} \dot{\sigma}_{n|n'n'} = & \left[i \nu (n'-n) - A \right] \sigma_{n|n'n'} \\ & + i \frac{\mu E_0}{2 \hbar} (\sigma_{n|n'n'} - \sigma_{non'o}) \\ & - \frac{\mu E_0}{2 \hbar} k_x \sqrt{\frac{\hbar}{2 \nu M}} \left[\sqrt{n} \sigma_{(n-1)|n'n'} + \sqrt{n+1} \sigma_{(n+1)|n'n'} \right. \\ & \left. + \sqrt{n'} \sigma_{n|(n'-1)o} + \sqrt{n'+1} \sigma_{n|(n'+1)o} \right] \end{aligned} \quad (52d)$$

These equations for $\sigma_{nm}n'm'$ correspond to the equations for the time evolution of the density matrix in Reference (11) when the assumptions made here are applied there. These equations of motion for the density matrix elements can possibly be solved numerically to determine the cooling rate for any parameters, and the fluorescence at any point during cooling.

IV. Conclusion

In summary, the problem of ion motion and laser cooling in a radio frequency quadrupole trap has been considered. An effective potential solution for the ion's wave function has been derived starting with the full time varying potential in Schrodinger's equation. The solutions for the total wave function include a phase factor, Θ , which does not appear in previous solutions. The effect of this phase factor is to cause transitions between the $n=N$ and $n=N \pm 2$ harmonic oscillator levels of the particle in the trap. It is argued that these transitions are weak and can be neglected for values of the frequency of oscillation of the electric field, Ω sufficiently greater than the resonant frequency, Ω_0 .

A wave packet solution to Schrodinger's equation with the time varying potential is presented. An equation for the width of the wave packet is derived. It is shown numerically that for $\Omega = 1.9 \Omega_0$ the width of the packet stays close to the initial value of the width, for $\Omega = 10 \Omega_0$ the width of the packet oscillates by an even smaller portion of the initial width, and for $\Omega = \Omega_0$ the width of the packet increases by at least two orders of magnitude. This behavior of the packet's width was taken as confirmation of the unimportance of transitions for values of Ω greater than Ω_0 .

The Hamiltonian matrix elements have been derived for a

trapped ion with two electronic levels in the presence of laser cooling. The matrix elements are derived for the Lambe-Dicke limit. When the laser is tuned below the electronic transition frequency, ω_0 by an amount ν , corresponding to the harmonic oscillator energy spacing, the combination of induced and spontaneous transitions causes a decrease in the harmonic oscillator quantum number. It was noted that when the ion reaches the ground state of the harmonic oscillator a decrease in the observed fluorescence should be seen, in some cases.

The equations of motion for the density matrix have been derived using the Hamiltonian matrix elements in the Lambe-Dicke limit. These equations are coupled and will have to be solved numerically. Such a numerical solution is planned, and the results, if available, will be used to determine the rate of cooling in the Lambe-Dicke limit and to gauge the change in fluorescent intensity when the ion reaches the ground state of the harmonic oscillator levels.

Bibliography

1. Blanch, Gertrude. "Mathieu Functions," Handbook of Mathematical Functions With Formulas, Graphs, and Mathematical Tables, edited by Milton Abramowitz and Irene A. Stegun. Washington, D. C.: U. S. Government Printing Office, 1964.
2. Cook, R. J. "Theory of Resonance Radiation Pressure," Physical Review A, 22: 1078-1098 (September 1980).
3. Cook, R. J. "Quantum-Mechanical Fluctuations of the Resonance-Radiation Force," Physical Review Letters, 44: 976-979 (14 April 1980).
4. Cook, R. J., D. G. Shankland, and A. L. Wells. "Quantum Theory of Particle Motion in a Rapidly Oscillating Field," Physical Review A (To be published).
5. Corliss, C. H. and W. R. Bozman. Experimental Transition Probabilities for Spectral Lines of Seventy Elements. Washington, D. C.: U. S. Government Printing Office, 1962.
6. Dehmelt, H. G. "Radio Frequency Spectroscopy of Stored Ions I: Storage," Advances In Atomic and Molecular Physics, Volume 3, edited D. R. Bates. New York: Academic Press, 1967.
7. Gordon, J. P. and A. Ashkin. "Motion of Atoms in a Radiation Trap," Physical Review A, 21: 1606-1617 (May 1980).
8. Hamming, R. W. Numerical Methods for Scientists and Engineers. New York: McGraw-Hill Book Company, Inc., 1962.
9. Itano, W. M. and D. J. Wineland. "Laser Cooling of Ions Stored in Harmonic and Penning Traps," Physical Review A, 25: 35-54 (January 1982).
10. Javanainen, J. "Light-Induced Motion of Trapped Ions I: Low-Intensity Limit," Journal of Physics B, 14: 2519-2534 (1981).
11. Javanainen, J., M. Lindberg, and S. Stenholm. "Laser Cooling of Trapped Ions: Dynamics of the Final Stages,"

Journal of the Optical Society of America B, 1:
111-115 (March 1984).

12. Landau, L. D. and E. M. Lifschitz. Mechanics.
Oxford: Pergamon, 1960.
13. Milonni, P. W. "Semiclassical and Quantum-Electrodynamical
Approaches in Nonrelativistic Radiation Theory,"
Physics Reports (1976).
14. Murphy, G. Ordinary Differential Equations and Their
Solutions. Princeton, New Jersey: D. Van Nostrand
Company, Inc., 1960.
15. Neuhauser, W., M. Hohenstatt, P. Toschek, and H. Dehmelt.
"Optical-Sideband Cooling of Visible Atom Cloud Confined
in Parabolic Well," Physical Review Letters, 41:
233-236 (24 July 1978).
16. Neuhauser, W., M. Hohenstatt, P. E. Toschek, and H.
Dehmelt. "Localized Visible Ba⁺ Mono-Ion
Oscillator," Physical Review A, 22: 1137-1140
(September 1980).
17. Reichl, L. E. A Modern Course in Statistical
Physics. Austin, Texas: University of Texas Press,
1980.
18. Wineland, D. J. and W. M. Itano. "Laser Cooling of
Atoms," Physical Review A, 20: 1521-1540 (October
1979).

Appendix: Computer Program for Numerically
Integrating Equations 17

```
10 ' Runge-Kutta Calculation
20 '
30 LET DT=.0001
40 LET F=2.
50 LET R=3.4344E-08
60 LET C=8.2594E+07
70 LET Y=2.9202E+07
80 LET Z=0.
90 LET T=0.
100 LPRINT DT, F, R, C
110 LET W=.0021511*SQR(1./Y)
120 LPRINT T, Y, Z, W
130 FOR N=1 TO 120
140 FOR K=1 TO 667
150 LET K11=DT*(2.*R*Y*Z)
160 LET K12=DT*(C*COS(F*T)+R*(Z^2-Y^2))
170 LET K21=DT*(2.*R*(Y+K11/2.)*(Z+K12/2.))
180 LET K22=DT*(C*COS(F*(T+DT/2.))+R*((Z+K12/2.)^2-(Y+K11/2.)^2))
190 LET K31=DT*(2.*R*(Y+K21/2.)*(Z+K22/2.))
200 LET K32=DT*(C*COS(F*(T+DT/2.))+R*((Z+K22/2.)^2-(Y+K21/2.)^2))
210 LET K41=DT*(2.*R*(Y+K31)*(Z+K32))
220 LET K42=DT*(C*COS(F*(T+DT))+R*((Z+K32)^2-(Y+K31)^2))
230 LET Y=Y+(1./6.)*(K11+2.*K21+2.*K31+K41)
240 LET Z=Z+(1./6.)*(K12+2.*K22+2.*K32+K42)
250 LET T=T+DT
260 NEXT K
270 LET W=.0021511*SQR(1./Y)
280 LPRINT T, Y, Z, W
290 NEXT N
300 END
```

Vita

Ann Laurie Wells was born on 21 December 1957 in Opelika, Alabama; the daughter of Claude and Diana Conn. She graduated from high school in LaFayette, Alabama in 1976. She attended Auburn University in Auburn, Alabama on a four year AFROTC Scholarship and a four year National Merit Scholarship. She received a Bachelor of Science in Physics with high honors and was commissioned in the Air Force on 6 June 1980. She was assigned to the Air Force Weapons Laboratory, Kirtland AFB, New Mexico where she worked with the Particle Beam Group, part of the Advanced Concepts Branch. In June 1983 she entered the Air Force Institute of Technology.

UNCLASSIFIED

SECURITY CLASSIFICATION OF THIS PAGE

AD-A163 838

REPORT DOCUMENTATION PAGE

1. REPORT SECURITY CLASSIFICATION UNCLASSIFIED			1b. RESTRICTIVE MARKINGS			
2a. SECURITY CLASSIFICATION AUTHORITY			3. DISTRIBUTION/AVAILABILITY OF REPORT Approved for public release; distribution unlimited.			
2b. DECLASSIFICATION/DOWNGRADING SCHEDULE						
4. PERFORMING ORGANIZATION REPORT NUMBER(S) AFIT/GEP/PH/84-12			5. MONITORING ORGANIZATION REPORT NUMBER(S)			
6a. NAME OF PERFORMING ORGANIZATION School of Engineering		6b. OFFICE SYMBOL (If applicable) AFIT/ENP		7a. NAME OF MONITORING ORGANIZATION		
6c. ADDRESS (City, State and ZIP Code) Air Force Institute of Technology Wright-Patterson AFB, Ohio 45433			7b. ADDRESS (City, State and ZIP Code)			
8a. NAME OF FUNDING/SPONSORING ORGANIZATION		8b. OFFICE SYMBOL (If applicable)		9. PROCUREMENT INSTRUMENT IDENTIFICATION NUMBER		
8c. ADDRESS (City, State and ZIP Code)			10. SOURCE OF FUNDING NOS.			
			PROGRAM ELEMENT NO.	PROJECT NO.	TASK NO.	WORK UNIT NO.
11. TITLE (Include Security Classification) See Box 19						
12. PERSONAL AUTHOR(S) Ann Laurie Wells, B.S., Capt, USAF						
13a. TYPE OF REPORT MS Thesis		13b. TIME COVERED FROM _____ TO _____		14. DATE OF REPORT (Yr., Mo., Day) 1984 December		15. PAGE COUNT 48
16. SUPPLEMENTARY NOTATION						
17. COSATI CODES			18. SUBJECT TERMS (Continue on reverse if necessary and identify by block number)			
FIELD	GROUP	SUB. GR.	Quantum Physics, Trapping, Ion Trapping, Laser Cooling, Lambe-Dicke Limit, Quadrupole Trap			
20	10					
19. ABSTRACT (Continue on reverse if necessary and identify by block number)						
Title: QUANTUM THEORY OF ION MOTION AND LASER COOLING IN A RADIO FREQUENCY QUADRUPOLE TRAP						
Thesis Chairman: Richard J. Cook, Major, USAF						
<div style="text-align: right;"> <p>Approved for public release: LAW AFB 190-1. <i>John E. Wolaver</i> JOHN E. WOLAVER 16 JAN 86 Dean for Research and Professional Development Air Force Institute of Technology (AFIT) Wright-Patterson AFB OH 45433</p> </div>						
20. DISTRIBUTION/AVAILABILITY OF ABSTRACT UNCLASSIFIED/UNLIMITED <input checked="" type="checkbox"/> SAME AS RPT. <input type="checkbox"/> DTIC USERS <input type="checkbox"/>			21. ABSTRACT SECURITY CLASSIFICATION UNCLASSIFIED			
22a. NAME OF RESPONSIBLE INDIVIDUAL Richard J. Cook, Major, USAF			22b. TELEPHONE NUMBER (Include Area Code) (513) 255-4498		22c. OFFICE SYMBOL AFIT/ENP	

The problem of ion motion and laser cooling in a radio frequency quadrupole trap is considered. It is shown by a simple numerical calculation that for ion motion in the absence of laser cooling the effect of the time varying potential $V(\vec{R})\cos\Omega t$ can be approximated by a time independent effective potential whenever the frequency of oscillation of the electric field, Ω is sufficiently greater than a resonant frequency, $\Omega_0 = \sqrt{2} eV_0/M$, where e is the electronic charge, V_0 is the maximum potential applied to the trap electrodes, and M is the mass of the ion.

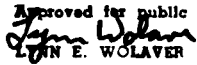
Equations for the Hamiltonian matrix elements in the presence of laser cooling, in the Lambe-Dicke limit are derived and studied to determine the cooling transitions. The equations of motion for the density matrix in the Lambe-Dicke limit are derived using a simple representation of spontaneous emission.

UNCLASSIFIED

SECURITY CLASSIFICATION OF THIS PAGE

AD-A163 838

REPORT DOCUMENTATION PAGE

REPORT SECURITY CLASSIFICATION UNCLASSIFIED			1b. RESTRICTIVE MARKINGS			
2a. SECURITY CLASSIFICATION AUTHORITY			3. DISTRIBUTION/AVAILABILITY OF REPORT Approved for public release; distribution unlimited.			
2b. DECLASSIFICATION/DOWNGRADING SCHEDULE						
4. PERFORMING ORGANIZATION REPORT NUMBER(S) AFIT/GEP/PH/84-12			5. MONITORING ORGANIZATION REPORT NUMBER(S)			
6a. NAME OF PERFORMING ORGANIZATION School of Engineering		6b. OFFICE SYMBOL (If applicable) AFIT/ENP		7a. NAME OF MONITORING ORGANIZATION		
6c. ADDRESS (City, State and ZIP Code) Air Force Institute of Technology Wright-Patterson AFB, Ohio 45433			7b. ADDRESS (City, State and ZIP Code)			
8a. NAME OF FUNDING/SPONSORING ORGANIZATION		8b. OFFICE SYMBOL (If applicable)		9. PROCUREMENT INSTRUMENT IDENTIFICATION NUMBER		
8c. ADDRESS (City, State and ZIP Code)			10. SOURCE OF FUNDING NOS.			
			PROGRAM ELEMENT NO.	PROJECT NO.	TASK NO.	WORK UNIT NO.
11. TITLE (Include Security Classification) See Box 19						
12. PERSONAL AUTHOR(S) Ann Laurie Wells, B.S., Capt, USAF						
13a. TYPE OF REPORT MS Thesis		13b. TIME COVERED FROM _____ TO _____		14. DATE OF REPORT (Yr., Mo., Day) 1984 December		15. PAGE COUNT 48
16. SUPPLEMENTARY NOTATION						
17. COSATI CODES			18. SUBJECT TERMS (Continue on reverse if necessary and identify by block number)			
FIELD	GROUP	SUB. GR.	Quantum Physics, Trapping, Ion Trapping, Laser Cooling, Lambe-Dicke Limit, Quadrupole Trap			
20	10					
19. ABSTRACT (Continue on reverse if necessary and identify by block number)						
Title: QUANTUM THEORY OF ION MOTION AND LASER COOLING IN A RADIO FREQUENCY QUADRUPOLE TRAP						
Thesis Chairman: Richard J. Cook, Major, USAF						
<p style="text-align: right;">Approved for public release: LAW AFB 190-1.  LYNN E. WOLAVER 16 JAN 86 Dean for Research and Professional Development Air Force Institute of Technology (AFIT) Wright-Patterson AFB OH 45433</p>						
20. DISTRIBUTION/AVAILABILITY OF ABSTRACT UNCLASSIFIED/UNLIMITED <input checked="" type="checkbox"/> SAME AS RPT. <input type="checkbox"/> DTIC USERS <input type="checkbox"/>			21. ABSTRACT SECURITY CLASSIFICATION UNCLASSIFIED			
22a. NAME OF RESPONSIBLE INDIVIDUAL Richard J. Cook, Major, USAF			22b. TELEPHONE NUMBER (Include Area Code) (513) 255-4498		22c. OFFICE SYMBOL AFIT/ENP	

DD FORM 1473, 83 APR

EDITION OF 1 JAN 73 IS OBSOLETE.

UNCLASSIFIED

SECURITY CLASSIFICATION OF THIS PAGE

END

FILMED

3-86

DTIC